

Identification of Putative *Artemisia annua* ABCG Transporter Unigenes Related to Artemisinin Yield Following Expression Analysis in Different Plant Tissues and in Response to Methyl Jasmonate and Abscisic Acid Treatments

Ling Zhang · Xu Lu · Qian Shen · Yunfei Chen ·
Tao Wang · Fangyuan Zhang · Shaoyan Wu ·
Weimin Jiang · Pin Liu · Lida Zhang · Yueyue Wang ·
Kexuan Tang

Published online: 28 December 2011
© Springer-Verlag 2011

Abstract Artemisinin has attracted interest due to its medicinal value in treating malaria and its potential for use against certain cancers and viral diseases. Trichome density and capacity determine artemisinin content in *Artemisia annua* plants. Thus, the ATP-binding cassette transporter G (ABCG) subfamily involved in trichome cuticle development may also influence artemisinin accumulation. In this study, putative *A. annua* ABC transporter unigenes were identified and classified from the unigene sequences up to date in the National Center for Biotechnology Information database, and nine putative *A. annua* ABCG transporter unigenes that may be involved in cuticle development were selected for expression analyses. Two of them, *AaABCG6* and *AaABCG7*, showed parallel expression pattern as two artemisinin biosynthesis-specific genes (amorpha-4, 11-diene synthase and a cytochrome P450-dependent hydroxylase, CYP71AV1) in different tissues and different leaf development stages and also showed similar induction in the plants after methyl jasmonate or abscisic acid treatments. Identification of these putative *A. annua* ABCG transporter unigenes could provide the basis for cloning of the full-length genes and further functional investigation to find the artemisinin relevant transporters, which could be used for

improving artemisinin yield in both *A. annua* plants and heterologous systems using transgenic technology.

Keywords ABCG transporter · *Artemisia annua* · Artemisinin · ADS · CYP71AV1 · Trichome cuticle

Introduction

Artemisinin is a sesquiterpenoid isolated from *Artemisia annua* L. plants. The therapies based on artemisinin are right now the most effective treatment against malaria, which causes 300–500 million cases and at least one million deaths annually (Graham et al. 2010; Milhous and Weina 2010). Artemisinin also showed potential as treatment for certain cancers and viral diseases (Efferth 2007; Efferth et al. 2008). Many works of fermentative production of artemisinin precursors through microbes have been developed (Arsenault et al. 2008; Chang et al. 2007; Ro et al. 2006; Zeng et al. 2008), but the traditional resource from *A. annua* plants would still be valuable for improving the yield of artemisinin (Covello 2008; Graham et al. 2010; Maes et al. 2010; Milhous and Weina 2010).

According to the researches of many groups, it is well accepted that artemisinin is synthesized in ten-cell glandular trichomes and finally accumulated in the subcuticular space at the top of the trichomes, which is between the cell wall of secretory cells and the cuticle (Duke et al. 1994; Maes et al. 2010; Schramek et al. 2010). The precursor for artemisinin biosynthesis, isopentenyl phosphate (IPP), could be obtained

L. Zhang · X. Lu · Q. Shen · Y. Chen · T. Wang · F. Zhang ·
S. Wu · W. Jiang · P. Liu · L. Zhang · Y. Wang · K. Tang (✉)
Fudan-SJTU-Nottingham Plant Biotechnology R&D Center,
School of Agriculture and Biology, Shanghai Jiao Tong University,
Shanghai 200240, China
e-mail: kxtang1@yahoo.com

K. Tang
e-mail: kxtang@sjtu.edu.cn

from both plastid (MEP) and cytosol (MVA) pathway, then IPP is condensed to farnesyl diphosphate (FPP) by farnesyl diphosphate synthase (FPS) (Schramek et al. 2010). The first artemisinin-specific biosynthesis step is the conversion from FPP to amorpha-4, 11-diene, which is catalyzed by amorpha-4, 11-diene synthase (ADS) (Mercke et al. 2000; Wallaart et al. 2001). Amorpha-4, 11-diene is further hydroxylated to artemisinic alcohol and then oxidized to artemisinic aldehyde by a cytochrome P450-dependent hydroxylase, CYP71AV1 (CYP) (Teoh et al. 2006). Subsequently, the most important direct precursor for artemisinin, dihydroartemisinic acid (DHAA), is converted from artemisinic aldehyde via dihydroartemisinic aldehyde by two enzymes, artemisinic aldehyde Delta 11(13) reductase (DBR2) (Zhang et al. 2008) and aldehyde dehydrogenase 1 (ALDH1) (Teoh et al. 2009), respectively. At the same time, artemisinic acid (AA) is also synthesized from artemisinic aldehyde with the help of CYP and ALDH1 (Teoh et al. 2006, 2009). It has been suggested that the last steps of artemisinin biosynthesis, conversion from DHAA to artemisinin, are enzyme independent, and AA is converted to arteannuin B (AB) in a similar way (Brown and Sy 2004, 2007; Lommen et al. 2006, 2007). Olsson et al. found that most artemisinin-specific biosynthetic enzymes, such as ADS, CYP, ALDH1, and DBR2, are expressed exclusively in the two outer apical cells, while FPS transcripts could be found through the whole trichome cells, and the 1-deoxy-D-xylulose-5-phosphate reductoisomerase (DXR), which is in the MEP pathway for IPP production, is not expressed in the two outer apical cells but in the subapical cells, where chloroplasts exist (Olsson et al. 2009).

One of the recent focuses is placed on searching genes influencing artemisinin yield (Graham et al. 2010; Maes et al. 2010), and since engineering transporters is a very important strategy for manipulation of secondary metabolites (Oksman-Caldentey and Inzé 2004), identification of artemisinin yield relevant transporters would be very useful in engineering *A. annua* plants or the heterologous host to improve artemisinin production.

Plant ATP-binding cassette (ABC) transporters play very important roles in the transport of secondary metabolites, such as alkaloids, phenol, terpenoids, and wax (Rea 2007; Verrier et al. 2008; Yazaki 2005, 2006). ABCG subfamily transporters include WBC and PDR transporters. It was proven that some ABCG transporters are involved in the transport of terpenoids (Campbell et al. 2003; Jasiński et al. 2001) or cuticle development (Bird et al. 2007; Panikashvili and Aharoni 2008; Panikashvili et al. 2010, 2011; Pighin 2004) in plants, and some are induced in the engineered yeast that produced more artemisinin precursors (Ro et al. 2008). It is possible that some ABCG transporters are involved in *A. annua* glandular trichome cuticle development and/or play roles in the transport relevant to artemisinin biosynthesis and accumulation, so it would be promising to

screen artemisinin yield relevant transporters from the ABCG subfamily.

There is a large amount of *A. annua* cDNA and EST sequences from different libraries up to date, and the National Center for Biotechnology Information (NCBI) has integrated these data to a relative complete inventory of *A. annua* unigene sequences. There are many successful bioinformatic data mining works on *A. annua* (Dai et al. 2010; Zhang et al. 2011b) and other plants (Kim et al. 2011; Wang et al. 2011; Zhang et al. 2011a). Part of *A. annua* unigene sequences from trichome-specific or non-trichome library has been classified in the TrichOME database (Dai et al. 2010). In this study, the unigene sequences from the NCBI and TrichOME database were compared and integrated, and 340 putative ABC transporter sequences were selected. After classification, nine putative ABCG transporter sequences that may be involved in cuticle development were picked, and their expression in different tissues and in methyl jasmonate (MJ) or abscisic acid (ABA)-treated plants was analyzed and discussed for their relevance to artemisinin yield and transport.

Materials and Methods

Transporters Identification and Classification

A. annua unigene and EST sequences were obtained from NCBI and TrichOME database (<http://www.plantrichome.org>), and then they were compared with TCDB ABC transporter proteins, which were retrieved from the TCDB database (<http://www.tcdb.org>), using BLASTX with e-values of less than $1e-04$. The sequences with significant similarity to TCDB ABC transporter proteins were selected for further analysis.

The selected sequences were assembled with Vector NTI (Invitrogen) and then annotated and classified with the best match compared against UniprotKB ABC transporter proteins, which were retrieved from UniprotKB database (<http://www.uniprot.org>), through BLASTX with e-values of less than $1e-04$. The alignment of protein sequences of selected *A. annua* unigenes and ABCG transporters from other species was carried out with CLUSTAL X (1.81) using default parameters.

Plant Materials

The seeds of *A. annua* were obtained from the School of Life Sciences, Southwest University in Chongqing, People's Republic of China. Plants of *A. annua* were grown in soil in a growth room at 25°C under 16 h of light and 8 h of dark per day, and some of them were transferred to a green house and field after 4 to 6 weeks.

A. annua plants at the beginning of florescence after grown in the field for 5 months were selected for RNA

extraction and expression analyses. The plants' young buds (Bud0), mature leaves (Leaf), and stems and roots (Stem and Root) were collected from five plants and pooled separately. The buds not fully blossomed (Bud1) and the fully floresent flowers (Flower) were collected and mixed after 7 and 14 days, respectively, from the same plants. On the other hand, *A. annua* plants grown in the green house for 1 month, 35 to 45 cm height, were chosen for collecting leaves from different positions of the plants. The meristem and the first, second, third, fifth, seventh, and ninth leaves counted from the apical top (Meristem, Leaf1, Leaf2, Leaf3, Leaf5, Leaf7, Leaf9) were collected separately from the main stem of five different plants. Leaves were then pooled respectively for each sample. Half of each leaf was cut and mixed for RNA extraction and expression analyses, and the rest of the part of the same leaf was for metabolite measurement.

MJ and ABA Treatment

A. annua plants grown in the growth room for 8 weeks were treated with solutions of 100 μ M ABA, 100 μ M MeJA (Sigma Aldrich, USA), and distilled water as mock control. Five plants were used for each treatment, respectively. Leaves were collected randomly from the pooled plants before treatment (0 h) and at different time points after treatment (1, 3, 6, 12, and 24 h) for the gene expression analyses and artemisinin quantification.

Real-Time qPCR for Expression Analysis

RNA was extracted using TIANGEN RNA prep pure plant kit (TIANGEN Biotech, Beijing, China) following the manufacturer's instructions. cDNA was prepared with Prime-Script RT reagent kit (Perfect Real Time) (Takara, Shiga, Japan). Real-time qPCR was performed on Peltier Thermal Cycler PTC-200 PCR Machines with Chromo4 continuous fluorescence detector (Bio-Rad, Watford, UK) with SYBR Premix Ex Taq (Perfect Real Time) (Takara) and gene-specific primers (Table 1). *ACTIN* was used as the control gene to normalize the expression level. Procedures of qPCR were performed as described in our previous research (Lu et al. 2011). Relative gene expression was calculated based on $2^{-\Delta\Delta CT}$ comparative method (Livak and Schmittgen 2001).

Metabolite Quantification

Leaves of *A. annua* plants were pooled and freshly weighed, then frozen in liquid nitrogen and kept at -70°C up to 1 month. Metabolites were extracted by immersing the fresh or frozen samples in chloroform for 2 min, dried in fume hood, and then re-dissolved in methanol, or by ultrasonic treatment of 100 mg of ground dry sample with 1 mL of methanol directly. The following treatments and artemisinin

Table 1 Primers used in real-time qPCR for selected unigenes

AaABC1F1	GCACCAGGAGACCCTAAAAT
AaABC1R1	AAACAAAACGTATACCTCCACA
AaABC2F1	TCAAACACCAGATCTACCCC
AaABC2R1	CAACTAAATGCAGTATAAGTGACG
AaABC3F1	CGCAAATCACAGGTAAGGA
AaABC3R1	TCTATGCAATGGGAGAACTCA
AaABC4F2	AGCCTCTGAGAACCCTGTAGT
AaABC4R2	TCCATTACCAGCCGAGT
AaABC5F2	ACATCTAAGGGAGGTCAAGGT
AaABC5R2	AAGCACCATCCCTTCGTTA
AaABC6F1	AGCCAATAGCCATAAGTGAAA
AaABC6R1	TTGGAGTATCTCATTGCTGGT
AaABC7F1	TGGGGAGGTATCTGTAAATGG
AaABC7R1	GGTGATGAAGAGGTTTCGTCC
AaABC8F1	GTGTCCATTGAATCTTGAAGG
AaABC8R1	AAGTCCACGCTCCTTGATG
AaABC9F1	GAAGGATTGCGGTGATACA
AaABC9R1	GGTCATCAAAACAATGCGAA
AaActinF	CCAGGCTGTTCAGTCTCTGTAT
AaActinR	CGCTCGGTAAGGATCTTCATCA
AaADSF4	AATGGGCAAATGAGGGACAC
AaADSR4	TTTCAAGGCTCGATGAACTATG
AaCYPF4	CACCCTCCACTACCCTTG
AaCYPR4	GACACATCCTTCTCCCAGC

measurement were performed with HPLC-ELSD as mentioned in our previous works (Lu et al. 2011; Zhang et al. 2009). Furthermore, the DHAA was measured with GC-MS (AutoSystem XL GC/TurboMass MS, Perkin Elmer, USA), equipped with a DB-5MS capillary column (30 m long \times 0.25 mm internal diameter; 0.25 μ m particle size) under the following conditions: injection port temperature, 250°C ; carrier gas, He (99.999%) 1.0 mL/min; split ratio, 5:1; initial column temperature, 80°C (raised at $10^{\circ}\text{C}/\text{min}$ to 300°C and then maintained for 14 min); and ionization voltage, 70 eV. The DHAA was identified according to the mass spectrum described by Wallaart et al. (1999), and relative DHAA content was calculated from the peak areas.

Results

Identification and Classification of Putative ABC Transporter Unigenes

A. annua unigenes, consisting of 93,672 sequences, from the NCBI database were compared with TCDB ABC transporter proteins through BLASTX, thus resulting 459 sequences being found with significant similarity to ABC transporter proteins.

Since some unigene sequences were already classified in the TrichOME database, 67 *A. annua* sequences that were annotated as ABC transporters were retrieved from this database. The sequences from these two databases were integrated, and 340 putative ABC transporter sequences were selected and then classified by comparing with Uniprot database ABC transporter proteins through BLASTX (Table 2).

Since ABCG transporters involved in trichome cuticle development might also determine artemisinin production, 129 sequences that have the highest similarity to the ABCG subfamily were selected for screening artemisinin yield relative transporters. As we know in *Arabidopsis*, ABCG11, ABCG12, and ABCG13 are involved in cuticle development for wax and/or cutin transport (Bird et al. 2007; Panikashvili and Aharoni 2008; Panikashvili et al. 2010, 2011; Pighin 2004). So all the ABCG transporters close to them according to the phylogenetic tree described in previous researches (Sánchez-Fernández et al. 2001; Yazaki 2005), including ABCG11, ABCG12, ABCG13, ABCG15, and ABCG3, were targeted for screening artemisinin relative transporters. Nine putative *A. annua* ABCG transporter unigenes (*AaABCG1*~9) were selected for the following analyses due to their highest similarity to the five *Arabidopsis* ABCG transporters. The protein sequences of these unigenes were aligned with selected ABCG transporters from other species (Fig. 1), and significant similarity could be found between them.

Expression Analyses of Different Tissues and Leaf Development Stages

Expression of nine selected ABCG unigenes in different tissues was investigated through real-time qPCR (Fig. 2). The artemisinin biosynthesis-specific gene *ADS* and *CYP* were highly expressed in young buds (Bud0), lower in non-fully flowering buds (Bud1) and fully blossomed flowers (Flower), poorly expressed in mature leaves (Leaf) and stems (Stem), and hardly expressed in roots (Root). *AaABCG6* and

AaABCG7 got very similar expression pattern like *ADS* and *CYP*, except that they were slightly expressed in the roots. *AaABCG1* was also highly expressed in Bud0, Bud1, and Flower samples, but still kept a certain expression level in mature leaves and stems. *AaABCG4* was just highly expressed in Bud0, Bud1, and Flower samples as *ADS* and *CYP*, but its expression increased as the flower matures. *AaABCG2* and *AaABCG9* were also hardly expressed in the roots, while *AaABCG5* was almost expressed at the same level in all the tissues.

To dissect the expression dynamics of artemisinin biosynthesis genes and the selected ABCG transporter unigenes during leaf development, the expression of these genes in the meristem and the leaves at different nodal positions of the plant (first, second, third, fifth, seventh, and ninth leaves) was also analyzed through real-time qPCR. *AaABCG6*, *AaABCG7*, and *AaABCG4* were just highly expressed in meristems and very young leaves, and then their expression reduced quickly during leaf development, which was the same as *ADS* and *CYP* (Fig. 3a). The other six candidates show some different patterns (Fig. 3b), or even a reverse pattern as *ADS* and *CYP* (Fig. 3c). Artemisinin and DHAA content in these leaves was also measured, respectively (Fig. 3d, e), suggesting that DHAA was accumulated rapidly during the early stage of leaf development (Meristem, Leaf1, Leaf2, Leaf3), when biosynthesis genes *ADS* and *CYP*, as well as the putative ABCG transporter unigenes *AaABCG6*, *AaABCG7*, and *AaABCG4*, were highly expressed, and then DHAA declined as the leaves aged, while the expression of *ADS*, *CYP*, *AaABCG6*, *AaABCG7*, and *AaABCG4* reduced simultaneously. On the other hand, from the beginning of leaf initiation, artemisinin content increased continuously up to a platform in the seventh and ninth leaves.

Expression Analyses After MJ and ABA Treatment

MJ and ABA have great influence on plant growth (Demetriou et al. 2010; Tripathy et al. 2011; Zambounis et al. 2011), and since it was proven that MJ and ABA could induce artemisinin accumulation in *A. annua* plants (Lu et al. 2011; Maes et al. 2010), expression of the nine selected ABCG transporter unigenes as well as *ADS* and *CYP* was also analyzed in MJ- and ABA-treated samples, which were compared to water-treated mock samples, and the artemisinin levels were also measured in these samples (Fig. 4).

In a short time period (1 to 6 h), expression of *ADS* and *CYP* was inhibited significantly in mock samples, but maintained or induced slightly in ABA- and MJ-treated samples. Twelve hours after treatment, the expression of these two genes increased vigorously in all MJ-, ABA-, and mock-treated samples, up to about six- to tenfold of 0-h samples, except that the expression of *ADS* was stimulated up to 30-fold in mock samples.

Table 2 Classification of selected putative *A. annua* ABC transporter unigenes

ABC transporters subfamily	Number of selected unigenes
ABCA	4
ABCB	61
ABCC	37
ABCD	6
ABCE	4
ABCF	10
ABCG	129
ABCI	10
Uncharacterized and no hits found	79

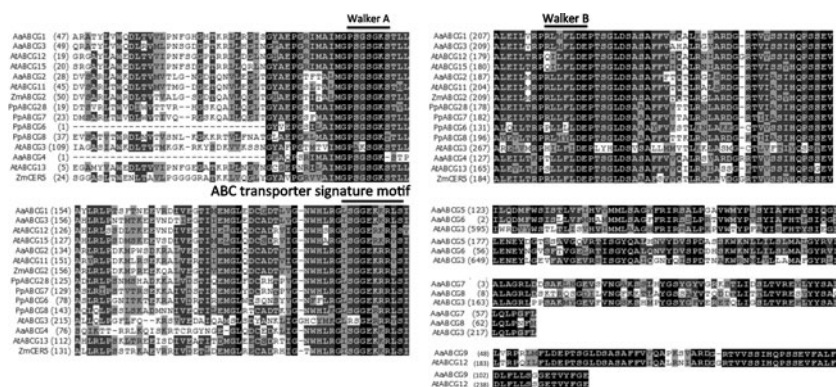


Fig. 1 The protein sequence alignment of selected AaABCG transporter unigenes with similar ABCG transporter from other species. The deduced amino acid sequence of AaABCG1 (Aan.97672, Aan.7512), AaABCG2 (Aan.29133), AaABCG3 (Aan.20798, Aan.21342), AaABCG4 (Aan.30350, Aan.32607, Aan.103542), AAABCG5 (Aan.67011), AaABCG6 (Aan.67737), AaABCG7 (Aan.68336), AaABCG8 (Aan.83267), AaABCG9 (Aan.70089, Aan.54903), and the protein sequence of AtABCG3 (Q9ZU9), AtABCG11 (Q8RXN0), AtABCG12 (Q9C8K2), AtABCG13 (Q9C8J8), AtABCG15 (Q8RWI9), ZmCER5

(ACG26663), ZmABCG2 (ACG25567), PpABCG6 (XP_001782413), PpABCG7 (EDQ59314), PpABCG8 (XP_001782003), and PpABCG28 (EDQ52515) were aligned with Clustal X program. The sequences marked with the *black bars* are the typical ABC transporter sequences. The sequences shown as *white color with black and dark gray background* indicate the completely identical and conservative residues, respectively, and the sequences shown as *black color with light gray background* indicate the similar residues

The expression of *AaABCG6* and *AaABCG7* was similar compared to *ADS* and *CYP*. Their expression was induced slightly (two- to threefold) after treated with ABA and MJ in a short time (3 to 6 h). At 12 h after treatments, expression of both of them was induced to six- to tenfold than 0-h samples in all the ABA-, MJ-, and mock-treated samples, except that *AaABCG7* expression was induced to around 18-fold in ABA-treated samples. *AaABCG4* got a similar pattern, though its expression was induced sharply up to 29-fold at 12 h after MJ treatment and was induced continuously up to 17-fold at 24 h after ABA treatment. All the other selected ABCG transporter unigenes got significant difference in induction pattern after treatments.

The artemisinin level was reduced in a short time (6 h) after mock treatment, but maintained at the same level or even higher in the ABA- or MJ-treated samples. Of all the treatment, the artemisinin content rose up significantly after 12 h (12, 24, and 48 h), which complied with the vigorous increase of expression of *ADS* and *CYP* at 12 h.

Discussion

In this work, the young trichome-specific pattern of artemisinin biosynthesis and the conversion process from DHAA to artemisinin in *A. annua* leaves were verified again. The meristem and the first, second, third, fifth, seventh, and ninth leaves on the main stem of *A. annua* plants are of the same type (not the leaves from leafy branches), so metabolites and gene expression analyses of these leaves could reflect the situation during leaf development. The expression pattern of *ADS* and *CYP* that was just highly expressed in the early stage

of leaf development (Fig. 3) and that was highly expressed in young trichome abundant tissues, such as young buds (Fig. 2), could verify the conclusions in previous works that most artemisinin biosynthesis genes are highly expressed during the early stage of trichome development (Graham et al. 2010; Olofsson et al. 2011). Lommen et al. showed that DHAA increases very fast after leaf appearance, then starts to convert to artemisinin later when the leaves are still rapidly expanding, the conversion continuing through the whole process of leaf development, even after the leaf starts senescence (Lommen et al. 2006). We got the same scenario in this study (Fig. 3d, e).

This work also verified that the expression of *ADS* and *CYP* would be inhibited by the release of artemisinin due to collapse of trichomes. Arsenault et al. proved that the expression of *ADS* and *CYP* would be inhibited by spraying the artemisinin or AA on the leaves of *A. annua* plants (Arsenault et al. 2010). They believed that a negative feedback of artemisinin and AA might exist on *ADS* and *CYP* genes. In this study, we also found that the expression of *ADS* and *CYP* was inhibited significantly in a short time in the water-sprayed samples (Fig. 4). It could be caused by artemisinin or AA released due to trichome collapse during water treatment and sample collection. Trichome collapse could also explain why artemisinin level declined rapidly in the mock-treated samples (Fig. 4).

MJ and ABA could induce artemisinin accumulation in both short and long periods after hormonal treatment. In the short time period, trichome collapse caused by water stress may lead to the loss of artemisinin and its precursors in all mock-, MJ-, and ABA-treated samples, but in MJ- and ABA-treated samples, expression of biosynthesis genes

and relative transporters was induced almost immediately, thus complementing the loss of precursors and artemisinin. This may explain why artemisinin content was maintained at the same level or even increased a little in the MJ- and ABA-treated samples. On the other hand, interestingly, the expression of *ADS* and *CYP* increased vigorously at 12 h in all mock-, ABA-, and MJ-treated samples, suggesting that this induction may not only be caused by ABA or MJ, but may also be due to the process of treatment and sample collection. We supposed that this sharp increase is stimulated by new trichome initiation. These results could explain why artemisinin content started to increase steadily after 12 h in all mock-, ABA-, and MJ-treated samples (Fig. 4).

There are some evidences which could support the existence of artemisinin biosynthesis relevant transporters. Firstly, artemisinin-specific biosynthesis genes *ADS*, *CYP*, *DBR2*, and

ALDH1 are expressed exclusively in the two outer apical cells, while the *DXR* in the MEP pathway is expressed in the subapical cells (Olsson et al. 2009). Based on these results and a $^{13}\text{CO}_2$ feeding experiment, Schramek et al. suggested that mixed IPP origin from both cytosol and plastid is condensed to a geranyl diphosphate (GPP) in subapical cells, then GPP is transported to apical cells and condensed to FPP with another IPP from the cytosol of apical cells (Schramek et al. 2010). It is reasonable that some transporters exist between apical and subapical cells of the glandular trichomes to transport the precursors to the location where artemisinin is synthesized. Secondly, since conversion from DHAA to artemisinin, as well as the process from AA to AB, is enzyme independent, while artemisinin is accumulated in the subcuticular space, it could also suggest that transporters are needed for transporting DHAA or AA to the final storage before their conversion to artemisinin or AB slowly. Besides the transporters involved in

Fig. 2 Expression of selected unigenes in different tissues of *A. annua* plants. Expression of *AaADS*, *AaCYP*, *AaABCG1*~*AaABCG9* in different tissues, including young buds (Bud0), buds not fully blossomed (Bud1), fully florescent flowers (Flower), mature leaves (Leaf), and stems and roots (Stem and Root), was measured through real-time qPCR. Values indicate the mean fold relative to sample Bud0. Error bars present SD (standard deviation) of three biological repeated samples

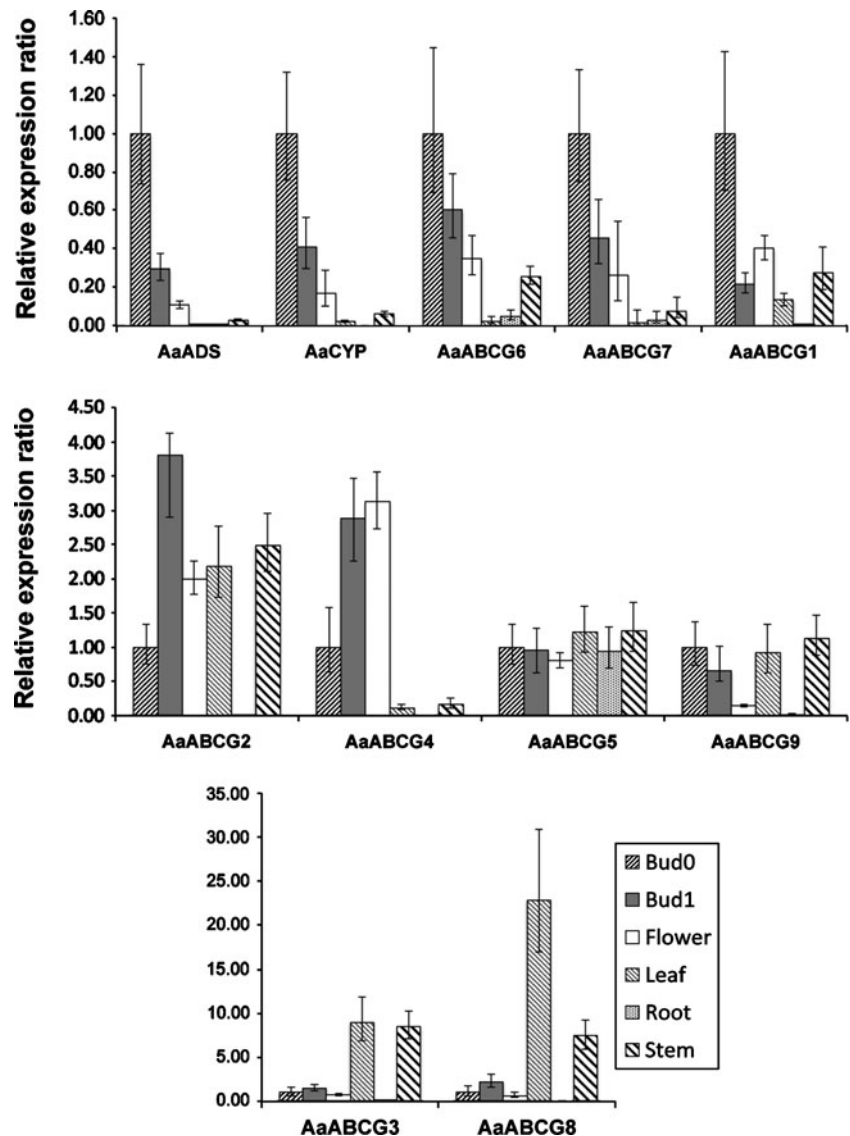
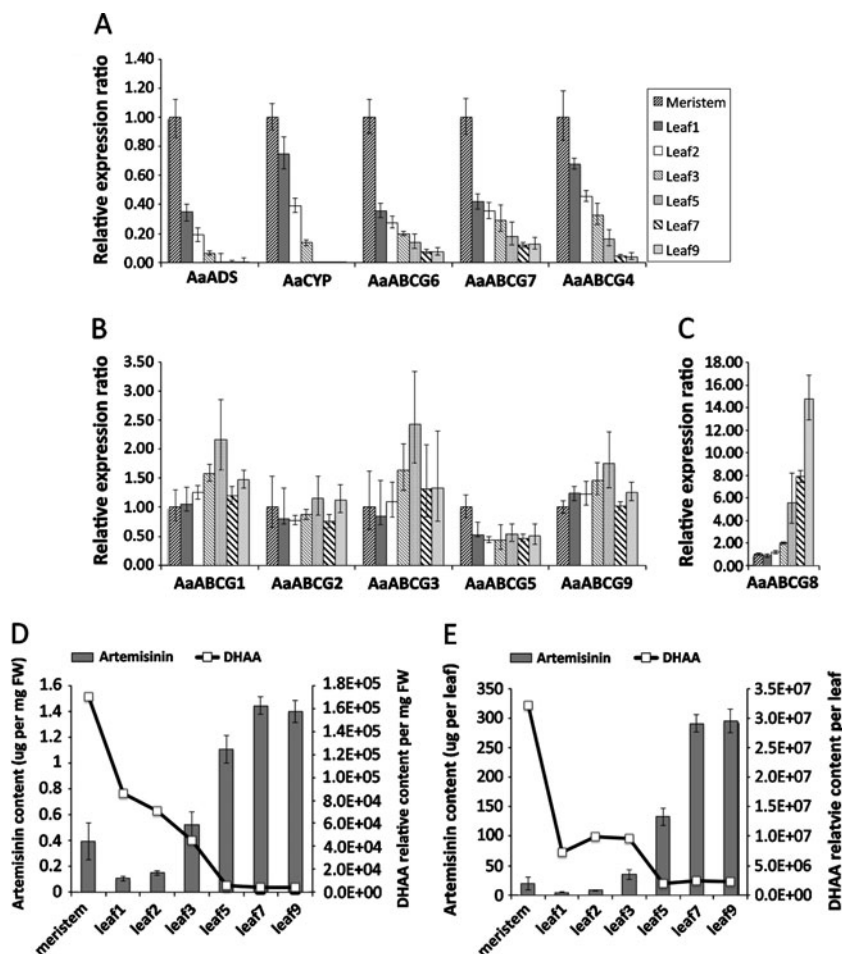


Fig. 3 Expression of selected unigenes and metabolite analyses in different leaves of *A. annua*. Expression of *AaADS*, *AaCYP*, and *AaABCG1* ~ *AaABCG9* in different leaves (Meristem, Leaf1, Leaf2, Leaf3, Leaf5, Leaf7, Leaf9) was measured through real-time qPCR (a–c). Values indicate the mean relative ratio of expression levels compared to sample Meristem. Error bars present SD (standard deviation) of three biological repeated samples. Artemisinin and dihydroartemisinic acid (DHAA) content per fresh weight (d) and per leaf (e) in different leaves of *A. annua* plants was measured by HPLC-ELSD and GC–MS, respectively. Columns show the mean values of artemisinin content. Lines with square dots show the relative content of DHAA. FW fresh weight. Error bars present SD (standard deviation) of three biological repeated samples



artemisinin biosynthesis, the transporters involved in trichome and cuticle development could also be relevant to artemisinin yield. Glandular trichome density and capacity were proven to be associated with artemisinin production (Lommen et al. 2006; Maes et al. 2010), so the transporters that influence trichome development may also determine artemisinin yield. Figure 5 showed the summary of the hypothetic artemisinin yield relevant transporters mentioned above.

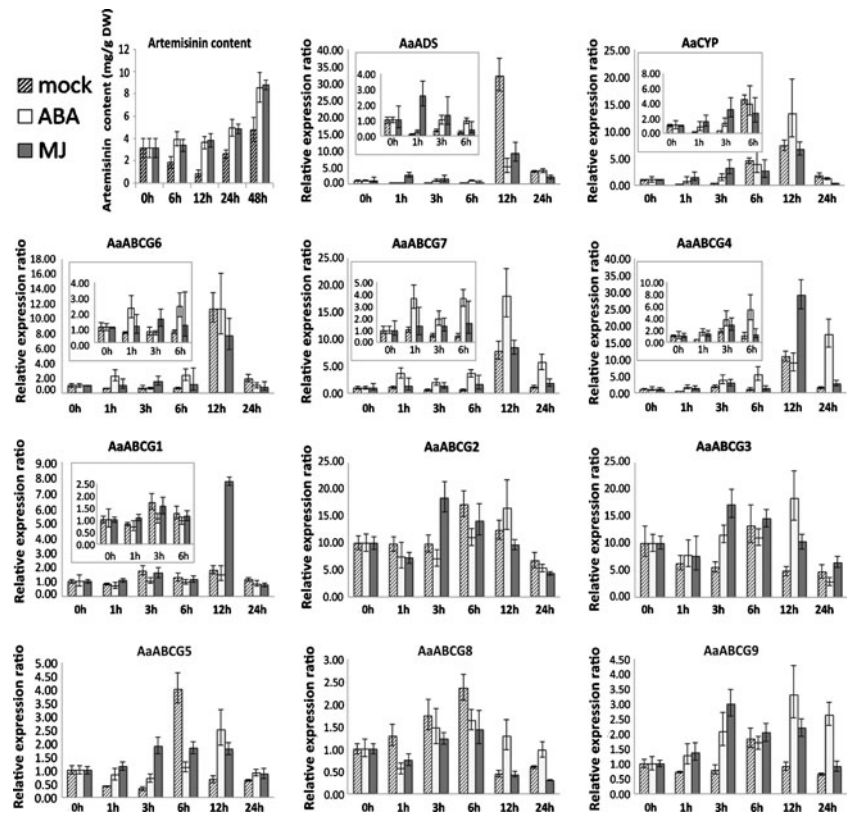
In this study, all the *A. annua* ABC transporter unigenes were classified, and nine putative ABCG transporter sequences that may be involved in cuticle development were selected for analyses. The results could provide primary support for the hypothesis of artemisinin yield relevant transporters mentioned in Fig. 5. Maes et al. cloned TFAR1, a trichome-specific fatty acyl-CoA reductase, and postulated that it is involved in cuticular wax formation during trichome development. This gene also has a similar trichome and young leaf-specific expression pattern as *ADS* and *CYP*, so they pointed out that a common mechanism for regulating metabolites and structure development of trichomes may exist (Maes et al. 2010). Similarly, in this work, *AaABCG6* and *AaABCG7* got parallel expression pattern as *ADS* and

CYP in the samples from different tissues (Fig. 2) and different leaf development stages (Fig. 3) and also got similar induction as *ADS* and *CYP* in the samples after water, ABA, and MJ treatments (Fig. 4). It could suggest that these two putative transporter unigenes may also share the same regulatory mechanism with artemisinin biosynthesis genes, thus are highly possible to be correlated to artemisinin yield. Though these two ABCG transporter unigene sequences are not the full-length cDNA, both of them got high similarity to *Arabidopsis* ABCG3 transporter, whose function has not been identified. It is likely that *AtABCG3* is also involved in secondary metabolite accumulation or trichome development. Besides *AaABCG6* and *AaABCG7*, some kind of similarity of expression pattern between *AaABCG1*, *AaABCG4*, and those two artemisinin-specific genes suggests that these putative transporters may also be relevant to artemisinin yield.

In summary, we identified and classified putative *A. annua* ABC transporter unigenes, and nine candidate ABCG transporter unigenes were selected for expression and metabolite analyses in different tissues and leaves from different development stages, as well as the samples after ABA

Fig. 4 Artemisinin content and expression of selected genes after different treatments.

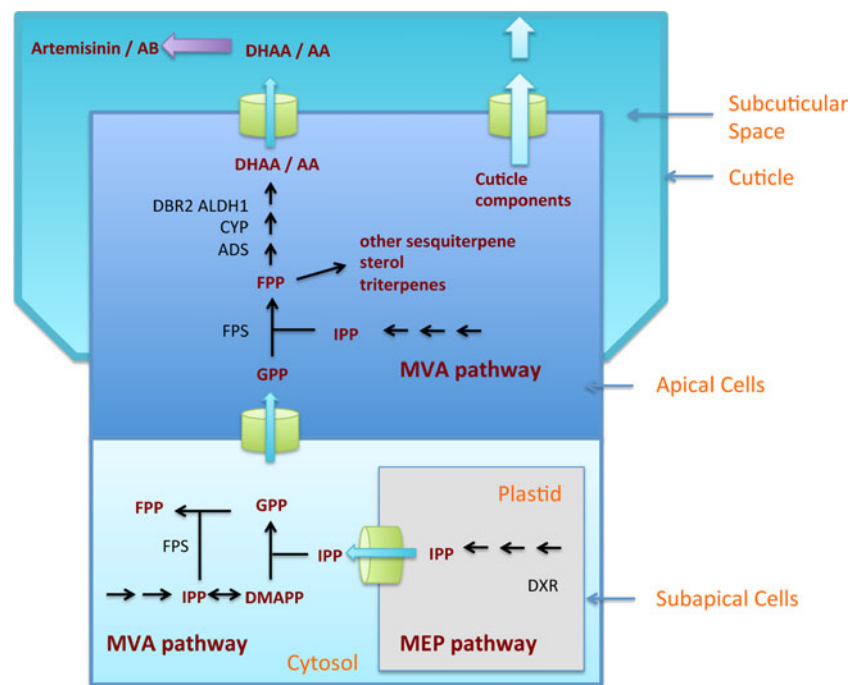
Expression of *AaADS*, *AaCYP*, and *AaABCG1~AaABCG9* in the leaves of plants before (0 h) and 1, 3, 6, 12, and 24 h after treated by mock, ABA, and MJ was measured through real-time qPCR. Values indicate the mean relative ratio of expression levels compared to sample 0 h. The artemisinin content of leaves from the same plants before (0 h) and 6, 12, 24, and 48 h after treated by mock, ABA, and MJ was measured by HPLC-ELSD method. Error bars present SD (standard deviation) of three biological repeated samples. DW dry weight



and MJ treatment. Two of them, *AaABCG6* and *AaABCG7*, have parallel expression patterns and may share the same regulatory system with artemisinin biosynthesis genes *ADS* and *CYP* and may have high relevance to artemisinin yield. Identification of these putative *A. annua* ABCG transporter

unigenes could provide the foundation for cloning the full-length genes and the further functional characterization to find artemisinin relevant transporters and then improving artemisinin yield in both *A. annua* plants and heterologous systems through transgenic technology.

Fig. 5 Putative transporters relevant to artemisinin yield. Transporters involved in artemisinin biosynthesis and cuticle development (illustrated as green cylinders) are shown as artemisinin yield relevant transporters. *IPP* isopentenyl phosphate, *GPP* geranyl diphosphate, *FPP* farnesyl diphosphate, *DHAA* dihydroartemisinic acid, *AA* artemisinic acid, *AB* arteannuin B, *DXR* 1-deoxy-D-xylulose-5-phosphate reductoisomerase, *FPS* farnesyl diphosphate synthase, *ADS* amorpha-4, 11-diene synthase, *CYP* amorpha-12-hydroxylase *CYP71AV1*, *DBR2* artemisinic aldehyde Delta 11(13) reductase, *ALDH1* aldehyde dehydrogenase 1



Acknowledgments This work was funded by China National High-Tech “863” Program (2011AA100605), Shanghai Science and Technology Committee (08391911800), and Shanghai Leading Academic Discipline Project (B209). We also thank the Instrumental Analysis Center of the Shanghai Jiao Tong University for assistance with the GC–MS analysis.

References

- Arsenault PR, Vail D, Wobbe KK, Erickson K, Weathers PJ (2010) Reproductive development modulates gene expression and metabolite levels with possible feedback inhibition of artemisinin in *Artemisia annua*. *Plant Physiol* 154:958–968
- Arsenault PR, Wobbe KK, Weathers PJ (2008) Recent advances in artemisinin production through heterologous expression. *Curr Med Chem* 15:2886–2896
- Bird D, Beisson F, Brigham A, Shin J, Greer S, Jetter R, Kunst L, Wu X, Yephremov A, Samuels L (2007) Characterization of *Arabidopsis* ABCG11/WBC11, an ATP binding cassette (ABC) transporter that is required for cuticular lipid secretion. *Plant J* 52:485–498
- Brown GD, Sy L-K (2004) In vivo transformations of dihydroartemisinic acid in *Artemisia annua* plants. *Tetrahedron* 60:1139–1159
- Brown GD, Sy L-K (2007) In vivo transformations of artemisinic acid in *Artemisia annua* plants. *Tetrahedron* 63:9548–9566
- Campbell EJ, Schenk PM, Kazan K, Penninckx IAMA, Anderson JP, Maclean DJ, Cammue BPA, Ebert PR, Manners JM (2003) Pathogen-responsive expression of a putative ATP-binding cassette transporter gene conferring resistance to the diterpenoid sclareol is regulated by multiple defense signaling pathways in *Arabidopsis*. *Plant Physiol* 133:1272–1284
- Chang MCY, Eachus RA, Triou W, Ro D-K, Keasling JD (2007) Engineering *Escherichia coli* for production of functionalized terpenoids using plant p450s. *Nat Chem Biol* 3:274–277
- Covello PS (2008) Making artemisinin. *Phytochemistry* 69:2881–2885
- Dai X, Wang G, Yang DS, Tang Y, Broun P, Marks MD, Sumner LW, Dixon RA, Zhao PX (2010) Trichome: a comparative omics database for plant trichomes. *Plant Physiol* 152:44–54
- Demetriou K, Kapazoglou A, Bladenopoulos K, Tsaftaris AS (2010) Epigenetic chromatin modifiers in barley: II. Characterization and expression analysis of the *HDA1* family of barley histone deacetylases during development and in response to jasmonic acid. *Plant Mol Biol Rep* 28:9–21
- Duke M, Paul R, Elsohly H, Sturtz G, Duke S (1994) Localization of artemisinin and artemisitenone in foliar tissues of glanded and glandless biotypes of *Artemisia annua* L. *Int J Plant Sci* 155:365–372
- Efferth T (2007) Willmar Schwabe Award 2006: antiparasitic and antitumor activity of artemisinin—from bench to bedside. *Planta Med* 73:299–309
- Efferth T, Romero MR, Wolf DG, Stamminger T, Marin JGG, Marschall M (2008) The antiviral activities of artemisinin and artesunate. *Clin Infect Dis* 47:804–811
- Graham IA, Besser K, Blumer S, Branigan CA, Czechowski T, Elias L, Guterman I, Harvey D, Isaac PG, Khan AM, Larson TR, Li Y, Pawson T, Penfield T, Rae AM, Rathbone DA, Reid S, Ross J, Smallwood MF, Segura V, Townsend T, Vyas D, Winzer T, Bowles D (2010) The genetic map of *Artemisia annua* L. identifies loci affecting yield of the antimalarial drug artemisinin. *Science* 327:328–331
- Jasiński M, Stukkens Y, Degand H, Purnelle B, Marchand-Brynaert J, Boutry M (2001) A plant plasma membrane ATP binding cassette-type transporter is involved in antifungal terpenoid secretion. *Plant Cell* 13:1095–1107
- Kim D-W, Kim RN, Choi S-H, Kim D-W, Nam S-H, Choi H-S, Koh HD, Kim A, Chae S-H, Ahn JC, Kang A, Park H-S (2011) EST analysis predicts putatively causative genes underlying the pharmaceutical application of *Glycyrrhiza uralensis* Fisch. *Plant Mol Biol Rep* 29:814–824
- Livak KJ, Schmittgen TD (2001) Analysis of relative gene expression data using real-time quantitative PCR and the $2^{-\Delta\Delta C(t)}$ method. *Methods* 25:402–408
- Lommen WJM, Elzinga S, Verstappen FWA, Bouwmeester HJ (2007) Artemisinin and sesquiterpene precursors in dead and green leaves of *Artemisia annua* L. *crops. Planta Med* 73:1133–1139
- Lommen WJM, Schenk E, Bouwmeester HJ, Verstappen FWA (2006) Trichome dynamics and artemisinin accumulation during development and senescence of *Artemisia annua* leaves. *Planta Med* 72:336–345
- Lu X, Lin X, Shen Q, Zhang F, Wang Y, Chen Y, Wang T, Wu S, Tang K (2011) Characterization of the jasmonate biosynthetic gene allene oxide cyclase in *Artemisia annua* L., source of the antimalarial drug artemisinin. *Plant Mol Biol Rep* 29:489–497
- Maes L, Van Nieuwerburgh FCW, Zhang Y, Reed DW, Pollier J, Vande Castele SRF, Inzé D, Covello PS, Deforce DLD, Goossens A (2010) Dissection of the phytohormonal regulation of trichome formation and biosynthesis of the antimalarial compound artemisinin in *Artemisia annua* plants. *New Phytol* 189:176–189
- Mercke P, Bengtsson M, Bouwmeester HJ, Posthumus MA, Brodelius PE (2000) Molecular cloning, expression, and characterization of amorpho-4,11-diene synthase, a key enzyme of artemisinin biosynthesis in *Artemisia annua* L. *Arch Biochem Biophys* 381:173–180
- Milhouse WK, Weina PJ (2010) Plant science. The botanical solution for malaria. *Science* 327:279–280
- Oksman-Caldentey K-M, Inzé D (2004) Plant cell factories in the post-genomic era: new ways to produce designer secondary metabolites. *Trends Plant Sci* 9:433–440
- Olofsson L, Engström A, Lundgren A, Brodelius PE (2011) Relative expression of genes of terpene metabolism in different tissues of *Artemisia annua* L. *BMC Plant Biol* 11:45. doi:10.1186/1471-2229-11-45
- Olsson ME, Olofsson LM, Lindahl A-L, Lundgren A, Brodelius M, Brodelius PE (2009) Localization of enzymes of artemisinin biosynthesis to the apical cells of glandular secretory trichomes of *Artemisia annua* L. *Phytochemistry* 70:1123–1128
- Panikashvili D, Aharoni A (2008) ABC-type transporters and cuticle assembly: linking function to polarity in epidermis cells. *Plant Signal Behav* 3:806–809
- Panikashvili D, Shi JX, Bocobza S, Franke RB, Schreiber L, Aharoni A (2010) The *Arabidopsis* DSO/ABCG11 transporter affects cutin metabolism in reproductive organs and suberin in roots. *Mol Plant* 3:563–575
- Panikashvili D, Shi JX, Schreiber L, Aharoni A (2011) The *Arabidopsis* ABCG13 transporter is required for flower cuticle secretion and patterning of the petal epidermis. *New Phytol* 190(1):113–124. doi:10.1111/j.1469-8137.2010.03608.x
- Pighin JA (2004) Plant cuticular lipid export requires an ABC transporter. *Science* 306:702–704
- Rea PA (2007) Plant ATP-binding cassette transporters. *Annu Rev Plant Biol* 58:347–375
- Ro D-K, Ouellet M, Paradise EM, Burd H, Eng D, Paddon CJ, Newman JD, Keasling JD (2008) Induction of multiple pleiotropic drug resistance genes in yeast engineered to produce an increased level of anti-malarial drug precursor, artemisinic acid. *BMC Biotechnol* 8:83. doi:10.1186/1472-6750-8-83
- Ro D-K, Paradise EM, Ouellet M, Fisher KJ, Newman KL, Ndungu JM, Ho KA, Eachus RA, Ham TS, Kirby J, Chang MCY, Withers ST, Shiba Y, Sarpong R, Keasling JD (2006) Production of the antimalarial drug precursor artemisinic acid in engineered yeast. *Nature* 440:940–943
- Sánchez-Fernández R, Davies TG, Coleman JO, Rea PA (2001) The *Arabidopsis thaliana* ABC protein superfamily, a complete inventory. *J Biol Chem* 276:30231–44

- Schramek N, Wang H, Römisch-Margl W, Keil B, Radykewicz T, Winzenhörlein B, Beerhues L, Bacher A, Rohdich F, Gershenzon J, Liu B, Eisenreich W (2010) Artemisinin biosynthesis in growing plants of *Artemisia annua*. A $^{13}\text{CO}_2$ study. *Phytochemistry* 71:179–187
- Teoh KH, Polichuk DR, Reed DW, Covello PS (2009) Molecular cloning of an aldehyde dehydrogenase implicated in artemisinin biosynthesis in *Artemisia annua*. *Botany* 87:635–642
- Teoh KH, Polichuk DR, Reed DW, Nowak G, Covello PS (2006) *Artemisia annua* L. (asteraceae) trichome-specific cDNAs reveal CYP71AV1, a cytochrome p450 with a key role in the biosynthesis of the antimalarial sesquiterpene lactone artemisinin. *FEBS Lett* 580:1411–1416
- Tripathy MK, Tyagi W, Goswami M, Kaul T, Singla-Pareek SL, Deswal R, Reddy MK, Sopory SK (2011) Characterization and functional validation of tobacco PLC Delta for abiotic stress tolerance. *Plant Mol Biol Rep*. doi:10.1007/s11105-011-0360-z
- Verrier PJ, Bird D, Burla B, Dassa E, Forestier C, Geisler M, Klein M, Kolukisaoglu U, Lee Y, Martinoia E, Murphy A, Rea PA, Samuels L, Schulz B, Spalding EJ, Yazaki K, Theodoulou FL (2008) Plant ABC proteins—a unified nomenclature and updated inventory. *Trends Plant Sci* 13:151–159
- Wallaart T, van Uden W, Lubberink H, Woerdenbag H, Pras N, Quax W (1999) Isolation and identification of dihydroartemisinic acid from *Artemisia annua* and its possible role in the biosynthesis of artemisinin. *J Nat Prod* 62:430–433
- Wallaart TE, Bouwmeester HJ, Hille J, Poppinga L, Majiers NC (2001) Amorpha-4,11-diene synthase: cloning and functional expression of a key enzyme in the biosynthetic pathway of the novel antimalarial drug artemisinin. *Planta* 212:460–465
- Wang W-K, Liu C-C, Chiang T-Y, Chen M-T, Chou C-H, Yeh C-H (2011) Characterization of expressed sequence tags from flower buds of alpine *Lilium formosanum* using a subtractive cDNA library. *Plant Mol Biol Rep* 29:88–97
- Yazaki K (2005) Transporters of secondary metabolites. *Curr Opin Plant Biol* 8:301–307
- Yazaki K (2006) ABC transporters involved in the transport of plant secondary metabolites. *FEBS Lett* 580:1183–1191
- Zambounis AG, Kalamaki MS, Tani EE, Paplomatas EJ, Tsiftaris AS (2011) Expression analysis of defense-related genes in cotton (*Gossypium hirsutum*) after *Fusarium oxysporum* f. sp. *vasinfectum* infection and following chemical elicitation using a salicylic acid analog and methyl jasmonate. *Plant Mol Biol Rep* doi:10.1007/s11105-011-0335-0
- Zeng Q, Qiu F, Yuan L (2008) Production of artemisinin by genetically-modified microbes. *Biotechnol Lett* 30:581–592
- Zhang D, Hu C, Ouyang Y, Yao J (2011a) Construction of a full-length cDNA library and analysis of expressed sequence tags from inflorescence of apomictic sabaigrass (*Eulaliopsis binata*). *Plant Mol Biol Rep*. doi:10.1007/s11105-011-0316-3
- Zhang H, Jin J, Tang L, Zhao Y, Gu X, Gao G, Luo J (2011b) Plantfdb 2.0: update and improvement of the comprehensive plant transcription factor database. *Nucleic Acids Res* 39:D1114–1117
- Zhang L, Jing F, Li F, Li M, Wang Y, Wang G, Sun X, Tang K (2009) Development of transgenic *Artemisia annua* (Chinese wormwood) plants with an enhanced content of artemisinin, an effective antimalarial drug, by hairpin-RNA-mediated gene silencing. *Biotechnol Appl Biochem* 52:199–207
- Zhang Y, Teoh KH, Reed DW, Maes L, Goossens A, Olson DJH, Ross ARS, Covello PS (2008) The molecular cloning of artemisinic aldehyde delta11(13) reductase and its role in glandular trichome-dependent biosynthesis of artemisinin in *Artemisia annua*. *J Biol Chem* 283:21501–21508